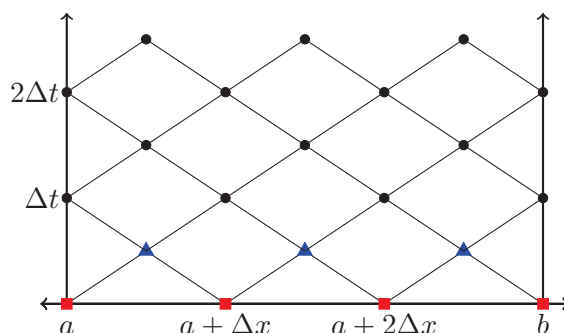


Copyright is owned by the Author of the thesis. Permission is given for a copy to be downloaded by an individual for the purpose of research and private study only. The thesis may not be reproduced elsewhere without the permission of the Author.

SYMPLECTIC INTEGRATORS  
FOR  
VAKONOMIC EQUATIONS  
AND FOR  
MULTI-HAMILTONIAN EQUATIONS



A THESIS PRESENTED IN PARTIAL FULFILMENT OF THE REQUIREMENTS FOR THE  
DEGREE OF  
DOCTOR OF PHILOSOPHY  
IN  
MATHEMATICS  
AT MASSEY UNIVERSITY, PALMERSTON NORTH,  
NEW ZEALAND.

Matthew Colin Wilkins

2016



# Contents

<b>Abstract</b>	<b>xiii</b>
<b>Acknowledgements</b>	<b>xv</b>
<b>1 Introduction</b>	<b>1</b>
1.1 Hamiltonian ODEs and PDEs . . . . .	2
1.2 Conservation laws and symmetry . . . . .	4
1.2.1 ODE conservation laws and symmetry . . . . .	5
1.2.2 PDE conservation laws and symmetry . . . . .	6
1.2.3 ODE symplectic conservation law . . . . .	8
1.2.4 PDE symplecticness . . . . .	13
1.3 Constrained Hamiltonian systems . . . . .	15
1.3.1 Numerical methods for constrained Hamiltonian ODEs . . . . .	17
1.4 Rationale for using symplectic methods . . . . .	19
1.5 General overview of this thesis . . . . .	21
<b>2 Constrained Hamiltonian systems</b>	<b>23</b>
2.1 Introduction to constrained Hamiltonian systems . . . . .	23
2.2 Symplectic integrators for generalized Hamiltonian systems . . . . .	30
2.3 Symplectic integrators for index 1 constraints . . . . .	34
2.4 Variational problems with holonomic and nonholonomic constraints . . . . .	35
2.5 Example: sub-Riemannian geodesics . . . . .	36
2.6 Example: the Heisenberg problem . . . . .	39
<b>3 The diamond scheme</b>	<b>43</b>
3.1 The simple diamond scheme . . . . .	46
3.2 The diamond scheme . . . . .	50
3.3 Dispersion analysis . . . . .	61
3.3.1 Dispersion relation for linear Schrödinger equation . . . . .	65
3.3.2 Stability of the simple and $r = 1$ diamond schemes . . . . .	67

<b>4</b>	<b>Diamond implementation</b>	<b>71</b>
4.1	Notation for diamond update equations . . . . .	71
4.2	Numerically solving diamond update equations . . . . .	74
4.2.1	Data structures . . . . .	76
4.3	Parallel diamond scheme . . . . .	77
<b>5</b>	<b>Diamond initialization and boundary treatment</b>	<b>83</b>
5.1	Diamond scheme initialization . . . . .	83
5.2	Numerical testing . . . . .	85
5.2.1	Schrödinger equation . . . . .	91
5.3	Dirichlet and Neumann boundary conditions . . . . .	93
<b>6</b>	<b>Conclusions</b>	<b>109</b>
6.1	Constrained Hamiltonian systems . . . . .	109
6.2	The diamond scheme . . . . .	111
6.3	Summary . . . . .	115
	<b>Bibliography</b>	<b>116</b>

# List of Tables

5.1	Numerical order, read off Figure 5.2, of the diamond scheme initialized with the exact solution and the diamond scheme initialization. It is apparent that for this problem the diamond initialization performs as well, or better, than the exact initialization. The order appears to be $r + 1$ for most $r$ (for $r = 4$ the order is $r + 2$ for some reason), whereas for the exact initialization the order is $r$ ( $r$ odd) and $r + 1$ ( $r$ even). . .	86
5.2	Sample problems. . . . .	86
5.3	Numerical order read from Figures 5.3–5.6 of the problems given in Table 5.2. To one significant figure the order appears to be $r$ , although in many cases it exceeds this. . . . .	91
5.4	Sample non-periodic problems. See Table 5.2 for the exact equations and solutions. The Dirichlet boundary conditions are found using the exact solution, and the Neumann conditions by differentiating the exact solution with respect to $x$ . Note there are no reasons, other than lack of resources/space/interest, for missing out the results for Esin D-N and Sine–Gordon D-N. . . . .	99
5.5	Numerical order read from Figures 5.11–5.16 for the problems given in Table 5.4. To one significant figure the order appears to be $r$ , although in some cases it exceeds this. . . . .	107



# List of Figures

1.1	The point $z$ is mapped forward to $\phi_t(z)$ , reflected about the line $p = 0$ , mapped back in time by $t$ , and finally reflected again in the $p = 0$ axis, arriving back at $z$ . . . . .	6
1.2	$u, v \in T_z\mathcal{M}$ , and their images under the flow $\phi$ . If the map, $\phi$ , is symplectic then the areas of the parallelograms are equal. . . . .	12
2.1	A two wheeled vehicle showing the front wheel angle $\phi$ and the vehicle angle of $\theta$ . . . . .	37
2.2	The energy error over time. This is the energy at each step minus the initial energy. The vehicle is trapped in the potential bowl $-V(\mathbf{q})$ , and the energy error does not show a linear growth in time. . . . .	38
2.3	Snapshots taken every fifth step of the two-wheeled vehicle starting at $(x, y, \theta, \phi, p_x, p_y, p_\theta, p_\phi) = (0.3, 0, 0, \pi, 0, 1.09, 1)$ , with $\Delta t = 0.1$ , and zero potential. The vehicle stays in a circle for many revolutions (not shown for clarity), but the geodesics is not stable, so eventually the vehicle wanders, as shown in the longer orbit on the right. The solutions for $p_\theta$ and $p_\phi$ suggest a relative homoclinic orbit. . . . .	39
2.4	The Heisenberg example starting at $(x, y, z, \dot{x}, \dot{y}, \dot{z}) = (0, 0, 0, 0.1, 0.3, 0)$ or $(x, y, z, p_x, p_y, p_z, \lambda) = (0, 0, 0, 0.1, 0.3, 1, 1)$ . Qualitatively the results look like [6, pg.14]. . . . .	41
3.1	The domain divided into diamonds by the simple diamond method. The solution, $z$ , is calculated at the corners of the diamonds. The scheme is started using the initial condition, which gives the solution along the $x$ axis at the red squares, and the solution at $t = \frac{\Delta t}{2}$ (the blue triangles) which is calculated using a forward Euler step (or the exact solution if known). After this initialization the simple diamond scheme proceeds, step by step, to update the top of a diamond using the other three known points in that diamond. . . . .	46
3.2	A single diamond in the simple diamond scheme. A diamond has a width of $\Delta x$ and height of $\Delta t$ . . . . .	47



3.3	The error of the simple diamond scheme applied to the multi-symplectic Hamiltonian PDE arising from the Sine–Gordon equation, and the error of the leapfrog scheme applied to the Sine–Gordon equation. The exact solution is the so-called <i>breather</i> on the domain $[-30, 30]$ . The Courant number is fixed at $\frac{1}{2}$ as $\Delta t$ , is decreased. Both methods appear to have order 2. . . . .	49
3.4	Solution of the linear wave equation on $[a, b]$ with Dirichlet boundary condition $u(a, t) = \sin a \cos t$ , Neumann boundary condition $u_x(b, t) = -\cos a \cos t$ , $a = 0.5$ , $b = \pi/2$ , and exact solution $u(x, t) = \sin x \cos t$ which contains both left- and right-moving waves. There are $N = 40$ diamonds in space and the Courant number is 0.5; 150,000 time steps are shown. See text for the handling of the boundary conditions. (i): phase portrait of $(u(b, t), v(b, t))$ , which is a circle in the exact solution. (ii): close-up of (i) showing some blurring of the orbit, which does not increase in time. (iii): Evolution of local energy $u(b, t)^2 + v(b, t)^2$ at $x = b$ vs. time (exact value is 1); the error does not increase in time. (iv): Global error in $u(b, t)$ vs. time. The error does not increase in time. (Note that $u(b, t)$ is not fixed by the boundary condition.) . . . . .	51
3.5	Information flows upwards as indicated by the solid blue arrows for a typical diamond. The solution, $z$ , is initialized on the solid blue zig-zag line. A step of the diamond scheme consists of two half-steps. The first half-step calculates $z$ along the green dash-dot line, which by periodicity is extended to the dashed line to the right. The second half-step uses the green dash-dot line to calculate the red dash-double-dotted line, which again by periodicity is extended to the left-hand dashed segment. . . . .	52
3.6	The diamond transformed by a linear transformation, $\Phi$ , to the unit square. The square contains $r \times r$ ( $r = 3$ in this example) internal stages, $Z_i^j$ . The solution is known along the bottom and left-hand sides. The method proceeds as two sets of $r$ Gauss Runge–Kutta $r$ -step methods: internal stage values, $Z_i^j$ , $X_i^j$ , $T_i^j$ , are calculated, then the right and top updated. . . . .	54
3.7	How the minimum singular value of $B$ varies with different Courant numbers. Because there are no zero singular values, the diamond scheme is solvable for the wave equation for all $\lambda \in [0, 1]$ and $r$ up to 5. It is easy to check this holds for larger $r$ . . . . .	57

3.8	The $r = 1$ diamond mesh, shown with $(\tilde{j}, \tilde{n})$ coordinate axes. Because the solution is defined on the red stars and blue circles, which do not form a regular grid in $(\tilde{j}, \tilde{n})$ space, the ansatz solution is given by $\tilde{z}_{\tilde{j}}^{\tilde{n}} = e^{i(\tilde{\mathcal{X}}\tilde{j} - \tilde{\Omega}\tilde{n})} c_1$ when $\tilde{n}$ is an integer (red stars), and $\tilde{z}_{\tilde{j}}^{\tilde{n}} = e^{i(\tilde{\mathcal{X}}\tilde{j} - \tilde{\Omega}\tilde{n})} c_2$ when $\tilde{j}$ is an integer (blue circles).	63
4.1	The domain divided into diamonds annotated with labels showing how each point is indexed. In this example $r = 2$ and there are only two diamonds across the domain. The points are indexed by diamond number counting from the left, leg number (0 for left leg, 1 for right leg), and finally point number, counting from the bottom. For example $[i, 1, j]$ is the $j$ th point from the bottom on the right leg of the $i$ th diamond. Because the boundary conditions are periodic the right-most green edge is considered the left edge of the left-most diamond.	76
4.2	Speed-up of the diamond scheme versus the number of cores for the code running on the NeSI Pan cluster. Code that was perfectly parallelizable would have the speed-up equal to the number of cores (the blue line). As the ratio of the number of cores to the amount of work (number of diamonds across the domain) increases one would expect the speed-up to deviate from the perfect blue line. In this region, though, the speed-up is very good.	79
4.3	Speed-up of the diamond scheme versus the number of cores for the code running on the NeSI Pan cluster. Code that was perfectly parallelizable would have the speed-up equal to the number of cores (the blue line). The number of diamonds across the domain is 1000, so at the maximum number of cores here, most cores have only two diamonds to work on. The overheads in communicating between cores is causing the speed-up to deviate from the perfect blue line. Note that the speed up was calculated from a single run (not an average of two runs) for the 450 and 499 number of cores runs.	80
5.1	The unit square under the map $x = \tilde{x} - \tilde{t}, t = \tilde{x}\tilde{t}$ .	83
5.2	The error of the diamond scheme initialized using the exact and diamond methods applied to the multisymplectic Hamiltonian PDE arising from the Sine–Gordon equation. The true solution was the so-called <i>breather</i> on the domain $[-30, 30]$ . The Courant number is fixed at $\frac{1}{2}$ as $\Delta t$ is decreased. For this problem the diamond initialization is equal or better than exact initialization.	85

5.3	The error of the diamond scheme with varying $r$ applied to the Esin problem (see Table 5.2). The Courant number is fixed at $\frac{1}{2}$ as $\Delta t$ is decreased. Table 5.3 summarizes the numerical order by reporting the slope of these lines. The numerical method cannot reduce the error any further than machine precision ( $\approx 10^{-16}$ for double floating point arithmetic). When the error has reached approximately machine precision, increasing $r$ and/or decreasing $\Delta t$ , just causes ‘noise’, and these parts of the error plot can be safely ignored. . . . .	87
5.4	The error of the diamond scheme with varying $r$ applied to the Sincos problem (see Table 5.2). See Figure 5.3 for general comments regarding these error plots. . . . .	88
5.5	The error of the diamond scheme with varying $r$ applied to the Coscos problem (see Table 5.2). See Figure 5.3 for general comments regarding these error plots. . . . .	89
5.6	The error of the diamond scheme with varying $r$ applied to the Sine–Gordon problem (see Table 5.2). At the larger values of $\Delta x$ and $\Delta t$ the error is not behaving as expected. However this is because $\Delta x$ and $\Delta t$ have not got small enough to cope with the much larger (than the other three problems) spatial domain. See Figure 5.3 for general comments regarding these error plots. . . . .	90
5.7	The error of the diamond scheme with $r = 1$ applied to the cubic nonlinear Schrödinger non-dimensionalized equation. $\frac{\Delta t}{\Delta x} = \frac{1}{2000}$ to keep $\Delta t < \frac{\Delta x^3}{24\sqrt{3}}$ over the range of $\Delta x$ . The error appears to be approximately order 2. . . . .	92
5.8	The energy from (5.7) for a cubic nonlinear Schrödinger non-dimensionalized $r = 1$ diamond scheme run. There are approximately 690,000 steps with $\Delta x = \frac{\pi}{8}$ and $\Delta t = \frac{1}{2} \frac{\Delta x^3}{24\sqrt{3}} \approx 0.0007$ . The energy error is large, but $\Delta x$ is large, so this is not surprising. The important fact is the energy error stays bounded. . . . .	94
5.9	A left-hand boundary phantom diamond in the $r = 2$ scheme. The solution, $z$ , is known at the circles on the SE edge. For an internal diamond, $z$ would also be known at the stars on the SW edge, but not in this case. Internally, nothing is known at the stars, and some information is known at the dashed circles. There needs to be enough known at these points marked with dashed circles to match the missing information on the SW stars. . . . .	96

5.10	An initial phantom diamond in the $r = 2$ scheme. The solution, $z$ , is not known on the SW or SE edges. Internally, nothing is known at the stars, and some information is known at the dashed circles. There needs to be enough known at these points marked with dashed circles to match the missing information on the SW and SE stars. . . . .	98
5.11	The error of the diamond scheme with varying $r$ applied to the Esin D-D problem (see Table 5.4). The Courant number is fixed at $\frac{1}{2}$ as $\Delta t$ is decreased. Table 5.5 summarizes the numerical order by reporting the slope of these lines. The numerical method cannot reduce the error any further than machine precision ( $\approx 10^{-16}$ for double floating point arithmetic). When the error has reached approximately machine precision, increasing $r$ and/or decreasing $\Delta t$ , just causes ‘noise’, and these parts of the error plot can be safely ignored. . . . .	100
5.12	The error of the diamond scheme with varying $r$ applied to the Sincos D-D problem (see Table 5.4). See Figure 5.11 for general comments regarding these error plots. . . . .	101
5.13	The error of the diamond scheme with varying $r$ applied to the Sincos D-N problem (see Table 5.4). See Figure 5.11 for general comments regarding these error plots. . . . .	102
5.14	The error of the diamond scheme with varying $r$ applied to the Coscos D-D problem (see Table 5.4). See Figure 5.11 for general comments regarding these error plots. . . . .	103
5.15	The error of the diamond scheme with varying $r$ applied to the Coscos D-N problem (see Table 5.4). See Figure 5.11 for general comments regarding these error plots. . . . .	104
5.16	The error of the diamond scheme with varying $r$ applied to the Sine–Gordon D-D problem (see Table 5.4). See Figure 5.11 for general comments regarding these error plots. . . . .	105
5.17	The error of the diamond scheme initialized with the diamond method (Section 5.1) and the boundary initialization method (Section 5.3), with varying $r$ applied to the Coscos D-N problem (see Table 5.4). The Courant number is fixed at $\frac{1}{2}$ as $\Delta t$ is decreased. The boundary initialization method is as good as, or better, than the diamond initialization method. . . . .	106



# Abstract

This thesis contains research contributions to two areas of geometric integration, one concerning ordinary differential equations (ODEs) and one concerning partial differential equations (PDEs).

The ODE contribution is a symplectic integrator for variational nonholonomic equations, also known as vakonomic equations. These systems include the Hamiltonian version of variational problems subject to position and velocity constraints that are nondegenerate in the velocities. Such constraints have the form  $g_i(q) \cdot \dot{q} = 0$ , and arise in sub-Riemannian geometry and control theory. An equivalence between variational equations with these constraints and generalized Hamiltonian systems of the form  $J\dot{z} = \nabla H(z)$  ( $J$  not necessarily invertible) with such index 1 constraints is shown. This is extended to constraints of the form  $g_i(q, \dot{q}) = 0$ . It is shown that symplectic Runge–Kutta methods are also symplectic on generalized Hamiltonian systems and provide effective symplectic integrators for Hamiltonian systems with index 1 constraints. Two sample applications are given: finding the motion of a two-wheeled idealized vehicle, and finding the geodesics of the Heisenberg group.

The PDE contribution is a new multisymplectic integrator. A class of general purpose linear multisymplectic integrators for multi-Hamiltonian equations based on a diamond-shaped mesh is introduced. The class of integrators consists of a *simple diamond scheme*, and a *diamond scheme* parameterized by order  $r$ . On each diamond, the former discretizes the PDE on the corners of the diamond, and the latter discretizes the PDE with  $r$ -stage symplectic Runge–Kutta methods. Both schemes advance in time by filling in each diamond locally, leading to greater efficiency and parallelization, and easier treatment of boundary conditions compared to methods based on rectangular meshes. The simple diamond scheme is order two in both space and time, has solvable equations for the one-dimensional wave equation, satisfies a discrete conservation law, and can be extended to allow Dirichlet and Neumann boundary conditions for the wave equation. The diamond scheme is defined on all multi-Hamiltonian PDEs, has solvable nonlinear equations for the one-dimensional wave equation, satisfies a discrete symplectic conservation law, and scales exceedingly well with the number of processors

on which it is run. A method for handling Dirichlet and Neumann boundary conditions is presented. Discrete dispersion relations, and associated stability results, are found for the wave equation and the cubic nonlinear Schrödinger equation. Numerical experiments, for both the simple diamond and  $r$  diamond schemes, are presented to support an estimate of the order of the schemes. Difficulties and complications, including boundary treatment and the multi-step nature of the diamond scheme, are discussed.

# Acknowledgements

This section was the most pleasurable to write: thinking of all the help I have received reminds me of how fortunate I am. I would not have been able to start this thesis without considerable support, let alone finish it.

First, of course, I thank my family. My parents for their support and upbringing. My brother, Andy, who: was always interested in knowing the details, asked insightful questions that made me think from a different perspective, and helped me with isoparametric coordinate transformations between triangles and diamonds. My kids who suffered having an absentee dad, especially when I was close to submitting. My wife, Heather, who not only had to put up with me doing less about the house, but also: proofread the entire thesis; checked all my articles and documents; listened to all my practice talks; put up with me grumbling about proofs that didn't work or code that was buggy; and made suggestions when I was stumped.

I started my PhD on a part-time basis while working at ITS Massey University. I am thankful to ITS, in particular Clive Martis, the CTO at the time, for allowing me to do this. ITS partially paid my fees, and allowed me time to meet with my supervisors.

In the first year of study my supervisor had two visitors: Klas Modin and Olivier Verdier. Both are very clever Mathematicians, but equally important to me, was that they were kind, clear, and willing to explain things to a slow, inexperienced student such as myself. Around that time we had the 'pre-magic conference' at Waikanae; that, and these two gentlemen really brought some life to the beginning of my PhD.

New Zealand eScience Infrastructure (NeSI) provided the parallel computing resources for me to test my code. The process, from requesting access to actually using a cluster, was straightforward and very smooth. NeSI clusters have an enormous amount of software (I didn't have to request a single package be installed!) and are staffed by knowledgeable and helpful people.

I was very thankful to be awarded a Massey Vice-Chancellor's Doctoral Scholarship. I could not have switched to full-time study without that ongoing money. Thank you to Simon Hall, head of IFS, for fostering a generous attitude within the institute towards PhD students, and authorizing the paying of my fees. Bruce van Brunt arranged part-time lecturing for me, not only did I appreciate the extra money, but greatly value the



experience this gave me.

In the course of my studies I got cancer. From my hospital bed, I emailed Kathryn Stowell asking her to be my champion and sort out all the paperwork and bureaucracy in changing from full-time back to part-time, and filing for a suspension. I have never been much for form filling at the best of times, so I very much appreciated what she did.

My co-supervisor, Stephen Marsland, is a busy person, but was always very generous with his time. When I was hopelessly lost, he took the time to explain things: I really appreciated learning what a tangent space really was. I enjoyed telling Stephen where I had got to in the project: explaining what I had been doing really helped in understanding where to go next. I am grateful for the Massey thesis L<sup>A</sup>T<sub>E</sub>X style and skeleton files that he created. Stephen read through the entire thesis in very short order and provided valuable feedback and improvements to the flow of this document.

Finally, I thank my supervisor Robert McLachlan. I could not have wished for a better supervisor. He took me on with no reservations, even though I had been out of academia for 15 years, and I quit half-way through my last attempt at a PhD! Robert has always been able to provide money for fees, conferences, and travel. He has been very generous with his encouragement and time, especially as I reached submission time. Robert was always happy to see me, and if necessary, provide commiserations and suggestions on what to try next. He always had an idea on how to rescue us from whatever mathematical hole I had managed to get us into!